

Heavy QCD Axion at Belle II: Displaced and Prompt Signals

Emilie Bertholet,¹ Sabyasachi Chakraborty,² Vazha Loladze,²
Takemichi Okui,^{2,3} Abner Soffer,¹ and Kohsaku Tobioka^{2,3}

¹*Tel Aviv University, School of Physics and Astronomy, Tel Aviv, 69978, Israel*

²*Department of Physics, Florida State University, Tallahassee, FL 32306, USA*

³*Theory Center, High Energy Accelerator Research Organization (KEK), Tsukuba 305-0801, Japan*

The QCD axion is a well-motivated addition to the standard model to solve the strong CP problem. If the axion acquires mass dominantly from a hidden sector, it can be as heavy as $O(1)$ GeV, and the decay constant can be as low as $O(100)$ GeV without running into the axion quality problem. We propose new search strategies for such heavy QCD axions at the Belle II experiment, where the axions are expected to be produced via $B \rightarrow Ka$. We find that a subsequent decay $a \rightarrow 3\pi$ with a displaced vertex leads to a unique signal with essentially no background, and that a dedicated search can explore the range $O(1-10)$ TeV of decay-constant values. We also show that $a \rightarrow \gamma\gamma$ can cover a significant portion of currently unexplored region of $150 \lesssim m_a \lesssim 500$ MeV.

I. INTRODUCTION

The axion is one of the most well-motivated hypothetical particles beyond the standard model (SM) of particle physics. The original axion was predicted by Weinberg and Wilczek [1, 2] as the pseudo-Nambu-Goldstone boson of the spontaneously broken $U(1)$ symmetry proposed by Peccei and Quinn [3, 4] to solve the strong CP problem [5]. While the axion could have additional couplings to the SM particles, the minimal effective Lagrangian thus motivated, up to terms to be included for renormalization, is given by

$$\mathcal{L} = \mathcal{L}_{\text{SM}} + \frac{\alpha_s}{8\pi} \frac{a}{f_a} G\tilde{G} + \frac{1}{2}(\partial_\mu a)^2 - \frac{m_a^2}{2}a^2, \quad (1)$$

where a is the axion, with mass m_a and decay constant f_a , and G is the gluon. Such an axion, which we call the *QCD axion*, is the subject of this paper.

Most phenomenological studies and experimental searches for the QCD axion have so far focused on *light* axion masses, i.e., $m_a < 3m_\pi$, where the physics is dominated by the axion-photon-photon coupling necessarily induced upon QCD confinement, even though the underlying Lagrangian (1) lacks such coupling. This coupling provides various experimental handles, such as the $a \rightarrow \gamma\gamma$ decay and the axion-photon conversion in a background magnetic field.

There are, however, good reasons to explore *heavy* axion masses, $m_a > 3m_\pi$, where hadronic physics controls the phenomenology. In particular, such a heavy QCD axion can provide a simple solution [6] to the *axion quality problem* [7–10], i.e., the violation of the $U(1)$ Peccei-Quinn symmetry by higher dimensional Planck-suppressed operators induced (presumably) by quantum gravity. Such violation should become harmless if $f_a \lesssim O(10)$ TeV [6], but this would imply $m_a \gtrsim O(1)$ keV due to the relation $m_a \sim m_\pi f_\pi / f_a$, if the axion mass is induced solely by QCD. This part of the parameter space, however, is excluded by beam dump experiments [11–13] and astrophysical observations [14–17]. The simplest way out is to introduce additional contributions to the axion

mass, such that $m_a \gg m_\pi f_\pi / f_a$ [6]. For our purpose, this simply amounts to treating m_a and f_a in the Lagrangian (1) as independent parameters. Such treatment can be justified by (small modifications of) many ultraviolet (UV)-complete models, such as those in Refs. [6, 18–21]. Also, a heavy QCD axion could be relevant to inflation, and in this case the interesting parameter is $m_a \sim 10^{-6} f_a$ [22].

In searching for a heavy QCD axion experimentally, the presence of the $aG\tilde{G}$ coupling in Eq. (1) implies that the predominant axion production should be hadronic. As a result, experiments such as proton beam dump [13, 23], kaon decays [24–32], precision measurements of pion decays [33–35], fixed target [23, 36, 37], and colliders [23, 38, 39] set strong bounds on f_a . For $m_a \gtrsim 50$ GeV the CMS dijet search excludes large regions of parameter space [40, 41].

On the other hand, the range $O(100)$ MeV $\lesssim m_a \lesssim 50$ GeV is poorly constrained. For $m_a > 400$ MeV the kaon and beam-dump experiments are not very effective, and in fact, the strongest probe to-date is from $B \rightarrow Ka$. The study of this channel was pioneered in Ref. [23], where the underlying $b \rightarrow sa$ amplitude was estimated and the branching fractions of the subsequent a decay into various final states were inferred by a data-driven method. The leading-order determination of the $b \rightarrow sa$ amplitude requires a 2-loop calculation and leading 2-loop renormalization group evolution with varying initial conditions for the evolution. This was performed in Ref. [42], where the result was combined with the data-driven branching fractions of [23] to derive constraints from the past B -factory results and future projections for Belle II for the prompt axion decays $a \rightarrow \pi^0\pi^+\pi^-$, $\eta\pi^+\pi^-$, $KK\pi$, and $\phi\phi$. Finally, axion production in $\phi \rightarrow \gamma a$ and $\eta' \rightarrow \pi\pi a$ also sets constraints on the parameter space [43].

In this paper, we aim to significantly extend the study of prospects of future searches at Belle II, which was discussed in Ref. [42]. In particular, we show that displaced axion decays to $\pi^0\pi^+\pi^-$ should provide a powerful search strategy, since the axion tends to be long-lived in the pa-

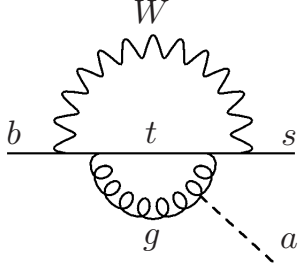


FIG. 1. A representative diagram of the leading contribution to the $b \rightarrow sa$ process from the Lagrangian (1).

parameter space of our interest, and hence this signature is associated with little background. The prompt and displaced axion decays $a \rightarrow \gamma\gamma$ is another promising signature to probe an allowed region at $m_a < 3m_\pi$. Since this channel was not explored in the previous work [42], we study its potential here.

II. SUMMARY OF $B \rightarrow K^{(*)}a$ THEORY CALCULATION

Here we summarize the theoretical results of Ref. [42]. From the Lagrangian (1), the leading contribution to the process $b \rightarrow sa$ arises at 2-loop order, a representative diagram being shown in Fig. 1. The $b \rightarrow sa$ amplitude is captured by the following effective operator at scales below M_W :

$$\mathcal{L}_{bsa} = C \frac{\partial_\mu a}{f_a} \bar{s}_L \gamma^\mu \gamma_5 b_L + \text{h.c.} \quad (2)$$

with

$$C = C_{bs}(\mu) + \frac{\alpha_w}{4\pi} C_{qq}(\mu) g(\mu) + \frac{1}{2} \frac{\alpha_w}{4\pi} \left(\frac{\alpha_s}{4\pi} \right)^2 f(\mu). \quad (3)$$

Here, $\mu \sim M_W$, and we refer the reader to Appendix B of Ref. [42] for the (lengthy) expressions of the functions $f(\mu)$ and $g(\mu)$. The coefficients $C_{qq}(\mu)$ and $C_{bs}(\mu)$ are required by renormalization of the 2-loop diagrams, the former being the coefficient of the $(\partial_\mu a/f_a) \bar{q} \gamma^\mu \gamma_5 q$ counterterm, and the latter being that of $(\partial_\mu a/f_a) \bar{s}_L \gamma^\mu \gamma_5 b_L$. Physically, these two coefficients parametrize the inevitably model-dependent effects of the UV physics that supersedes the low energy description, Eq. (1), above some high scale Λ_{UV} . Rather than committing to a particular UV model, Ref. [42] varies the “initial conditions”, $C_{qq}(\Lambda_{UV})$ and $C_{bs}(\Lambda_{UV})$, over their natural ranges and uses the renormalization group evolution of $C_{qq}(\mu)$ and $C_{bs}(\mu)$ to study the impact of the unknown UV physics on the bounds on m_a and f_a extracted in the infrared. To go from the $b \rightarrow sa$ amplitude to the $B \rightarrow K^{(*)}a$ branching fraction, the result above is then combined with form factors obtained from the light-cone QCD sum rules [44–47]. An approximate formula for the branching fraction

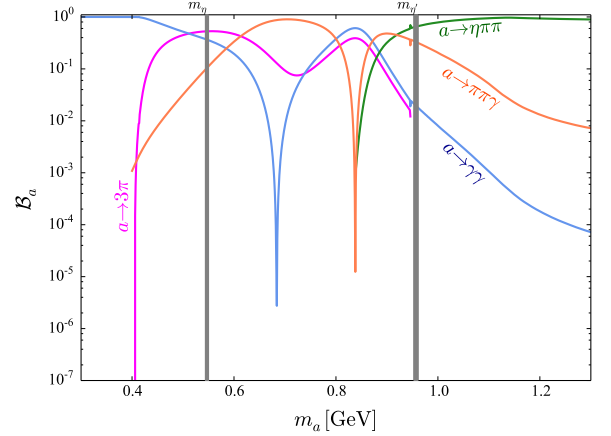


FIG. 2. Heavy QCD axion branching fractions as a function of its mass, taken from [23]. The decay modes relevant to our analyses are $a \rightarrow 3\pi$, $\gamma\gamma$, and $\eta\pi\pi$.

based on Eq. (8) of Ref. [42], with $A = +3$ and $B = -3$ is given by

$$\text{BR}(B^+ \rightarrow K^+ a) \simeq 2(10) \times 10^{-5} \left(\frac{100 \text{ GeV}}{f_a} \right)^2, \quad (4)$$

for $\Lambda_{UV} = 1(10)$ TeV, respectively.

III. AXION DECAYS: DISPLACED AND PROMPT

Due to its coupling to gluons, the decays of a heavy QCD axion are very diverse [23]. In terms of the ranges of m_a , we can summarize the decay patterns as follows.

For $3m_\pi < m_a < m_\eta + 2m_\pi \sim 900$ MeV, the branching fraction of $a \rightarrow 3\pi$ is sizable, as shown in Fig. 2. In this mass range, with f_a in the range of our interest $1 \lesssim f_a \lesssim 10$ TeV, the axion can give rise to a displaced vertex signature in the Belle II detector. Because of the displacement, one can optimize experimental cuts to reduce the background considerably. Consequently, analyzing displaced $B \rightarrow Ka(3\pi)$ can result in very strong bounds on f_a . For higher f_a the axion would be effectively invisible, a signature for which detection methods exist, but with very low efficiency [48]. Furthermore, as seen from Eq. (4), the production rate of the axion in this case is too small even with the full data set of Belle II. Hence, the channel $B \rightarrow Ka(\text{invisible})$ is unfavorable, unless other couplings than in Eq. (1) increase the axion production.

For $m_a > m_\eta + 2m_\pi$, the decay mode of $a \rightarrow \eta\pi\pi$ quickly dominates, and the axion lifetime becomes shorter. This channel was studied in Ref. [42].

For $m_a < 3m_\pi$, $a \rightarrow 2\gamma$ dominates.¹ Thus, to search

¹ $a \rightarrow \gamma\pi\pi$ is allowed, but its branching ratio is very small for

for a heavy QCD axion with mass below ~ 400 MeV one has to study the diphoton final state.

To summarize, in this paper, we present projections for the reach of Belle II using displaced $B \rightarrow Ka(3\pi)$ decays, and $B \rightarrow Ka(\gamma\gamma)$ decays that may be prompt or displaced.

A. Displaced $B^- \rightarrow K^- a(\pi^+\pi^-\pi^0)$ signature

In the mass range $3m_\pi < m_a < m_\eta + 2m_\pi$, we propose to search for the axion in $B^- \rightarrow K^- a$ with $a \rightarrow \pi^+\pi^-\pi^0$, where the two charged pions form a displaced vertex (DV) significantly away from the interaction point of the e^+e^- beams. Exploiting the DV signature results in large background suppression [49–52]. Given the already low level of background observed by the Belle Collaboration for the decay $B \rightarrow K\omega$ with $\omega \rightarrow \pi^+\pi^-\pi^0$ [53], we take the background in this search to be negligible.

To estimate the signal efficiency, we use EvtGen [54] to generate $B^- \rightarrow K^- a(\pi^+\pi^-\pi^0)$ events at the Belle II beam energies ($E_{e^-} = 7$ GeV and $E_{e^+} = 4$ GeV). We generate 1533 samples of 10k events each, with $m_a \in [450, 950]$ MeV and $f_a \in [1, 10^5]$ GeV, and calculate the effective efficiency for each sample, as follows. Following Refs. [55, 56], we define the detector fiducial volume to be a cylinder of length $-40 < z < 120$ cm along the beam direction and maximal radius $r < 80$ cm in the transverse plane, excluding the radial region $r < 1$ cm in order to reject the promptly produced tracks. If a generated axion decays outside of the fiducial volume, its contribution to the efficiency is 0. For decays inside the fiducial volume, the radius-dependent track-detection efficiency ϵ_{det} is taken to be linearly decreasing from $r = 1$ cm ($\epsilon_{\text{det}} = 100\%$) to $r = 80$ cm ($\epsilon_{\text{det}} = 0$) [55, 56]. Finally, to take into account overall detection and reconstruction efficiencies, we multiply the efficiency by an overall factor of 22%, which we estimate from the Belle study of $B \rightarrow K\omega$ [53], to obtain the total efficiency, ϵ_{tot} . The total signal efficiency as a function of mean decay length and the axion mass is plotted in Fig. 3.

B. Prompt $B^- \rightarrow K^- a(\gamma\gamma)$ signature

In the mass range $m_a < 3m_\pi \simeq 400$ MeV, the axion decays predominantly to $\gamma\gamma$. Furthermore, there is a range of allowed values of f_a for which the axion lifetime is less than a few centimeters, below the detector spatial resolution for the point of origin of a photon. We show in Fig. 4 that large part of this parameter space can be probed by Belle II in $B^- \rightarrow K^- a(\gamma\gamma)$, with displaced decays for the approximate mass ranges $m_a < 500$ MeV, and mostly prompt decays for $m_a > 500$ MeV. We take

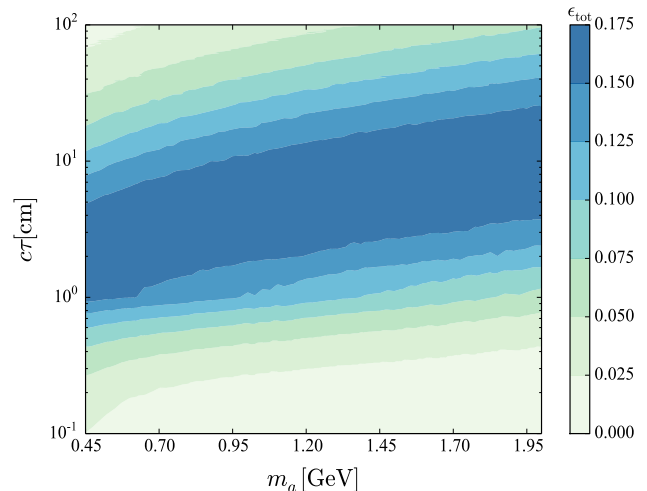


FIG. 3. We show contours of the total efficiency for the displaced $a \rightarrow \pi^+\pi^-\pi^0$ channel in the plane of axion mass and decay length. An overall factor of 22% has been included to account for the detection and reconstruction efficiencies [53].

the efficiency for this decay chain to be 38%, consistent with the efficiencies found by Belle [57] and BaBar [58] in the decays $B^- \rightarrow K^- \pi^0$ and $B^- \rightarrow K^- \eta(\gamma\gamma)$, respectively. For completeness, we also calculate the sensitivity of the diphoton mode for higher masses, for which one is sensitive only to prompt axion decays and other final states constitute better probes.

1. Background

We estimate the background at a benchmark value of the diphoton mass $m_{\gamma\gamma}$ around the η mass from the Belle study of $B^- \rightarrow K^- \eta$ [59]. The top-left plot of Fig. 3 of Ref. [59] shows a total of about 80 background events in the 4 bins centered on the signal peak, for a data sample of about 0.75 ab^{-1} in the diphoton mass range $501 < m_{\gamma\gamma} < 573$ MeV. This corresponds to a background level of about 70 events per MeV of $m_{\gamma\gamma}$ in the 50 ab^{-1} Belle II dataset. While the plot includes both $\eta \rightarrow \gamma\gamma$ and $\eta \rightarrow \pi^+\pi^-\pi^0$ events, Table 1 of Ref. [59] shows that the $\gamma\gamma$ final state accounts for most of the signal and background events. Therefore, we conservatively take this background yield to apply only to the $\gamma\gamma$ channel of interest. The background level decreases with $m_{\gamma\gamma}$. Around the D^0 mass it is smaller by about a factor of 3 relative to the above estimate. Somewhat conservatively, we ignore this effect, which has little impact on our sensitivity estimate. Similarly, the background is larger by about a factor of 5 for $m_{\gamma\gamma}$ values around the π^0 mass [60]. However, as discussed below, the sensitivity at low mass is limited by the axion lifetime and not by the background. Therefore, we ignore the background increase at low mass as well.

$m_a < 3m_\pi$. See the orange line of Fig. 2.

2. Mass Smearing

The background estimate must take into account the $m_{\gamma\gamma}$ resolution of the signal peak. For prompt axion decays, the relevant resolution ranges from $\sigma_{m_{\gamma\gamma}} \approx 11$ MeV for $m_{\gamma\gamma} \approx 540$ MeV [61] to $\sigma_{m_{\gamma\gamma}} \approx 35$ MeV for $m_{\gamma\gamma} \approx 1860$ MeV [62].

Displaced photons have an additional source of smearing: the angular resolution of the calorimeter is not sufficient for determining the point of origin of a photon. Therefore, the diphoton mass $m_{\gamma\gamma}$ must be calculated assuming that the photons are prompt. This results in a downward smearing of $m_{\gamma\gamma}$ equal to roughly $\sigma_{m_{\gamma\gamma}}^{\text{disp}} \sim (r/S)m_a$, where $r = ct_a p_a/m_a$ is the flight distance of an axion with decay time t_a and momentum p_a , and S is the distance from the interaction point to the face of the calorimeter at the relevant point. This linear relation holds for small values of r/S . Given the typical size of the Belle II calorimeter, $S = 120$ cm, we restrict our sensitivity estimate to average flight distances in the range $\langle r \rangle < 20$ cm, and use the estimated value for the smearing $\sigma_{m_{\gamma\gamma}}^{\text{disp}} \sim 0.2 m_a$. Given the rather low boost of the center-of-mass frame at Belle II, we ignore the momentum of the B meson when calculating p_a .

3. Mass Binning

For the purpose of estimating the search sensitivity, we estimate the signal and background yields in bins of $m_{\gamma\gamma}$. In the long-lived mass range, we take six bins with the bin boundaries $\{145, 160, 200, 250, 320, 400, 500\}$ MeV. Above 160 MeV, this corresponds to a bin width of approximately $\sigma_{m_{\gamma\gamma}}^{\text{disp}}$, given that the resolution for $m_{\gamma\gamma} < m_a$ is dominated by $\sigma_{m_{\gamma\gamma}}^{\text{disp}}$, which is much worse than the intrinsic detector resolution $\sigma_{m_{\gamma\gamma}}$, which dominates for $m_{\gamma\gamma} > m_a$. The lower boundary of $m_{\gamma\gamma} = 145$ MeV is about $2\sigma_{m_{\gamma\gamma}}$ from the π^0 mass peak, rejecting about 97% of the $B^+ \rightarrow K^+\pi^0$ background. Since Fig. 1 of Ref. [60] shows that the $B^+ \rightarrow K^+\pi^0$ event yield is only a few times that of the combinatorial background, this selection brings the $B^+ \rightarrow K^+\pi^0$ background down to negligible levels. Since the width of the bin $145 < m_{\gamma\gamma} < 160$ MeV is about $\sigma_{m_{\gamma\gamma}}^{\text{disp}}/2$, we take the efficiency in this bin to be reduced by a factor of 2.

In the prompt range of interest, $500 < m_a < 1300$ MeV, $\sigma_{m_{\gamma\gamma}}$ varies only between about 11 and 25 MeV, and the resolution asymmetry is much smaller [61, 62]. Therefore, we simplify the treatment and take a fixed bin width of 40 MeV. As seen in Fig. 4, this region contains islands around 600 MeV and particularly 800 MeV in which the axion is rather long-lived, reaching $c\tau \sim 10$ cm for $\Lambda_{\text{UV}} = 10$ TeV. Due to the relatively low boost in these regions, which implies $\langle r \rangle < 35$ cm, we ignore the impact of $\sigma_{m_{\gamma\gamma}}^{\text{disp}}$.

4. Sensitivity Estimate

For each value of m_a and f_a , we estimate the number N_S of signal events that satisfy $r < 20$ cm and the number N_B of background events scaled from Ref. [59]

that fall within the corresponding $m_{\gamma\gamma}$ bin. We take the sensitivity of the experiment to be the f_a value for which $N_S/\sqrt{N_B} > 2$. For $m_a < 500$ MeV, this naive estimation results in $\langle r \rangle$ values that are much smaller than 20 cm. To remove this inconsistency, we weaken the f_a sensitivity in this region to correspond to $\langle r \rangle = 20$ cm.

This treatment glosses over details of the experimental analysis, which we briefly discuss here. Given the high resolution and small bins for $m_{\gamma\gamma} > 500$ MeV, we expect the search to be performed by fitting the $m_{\gamma\gamma}$ spectrum for a signal peak plus a smooth background distribution. For $m_{\gamma\gamma} < 500$ MeV, the poor resolution and small number of bins suggest that the analysis should proceed by estimating the background in each bin by other methods. Since most photons originate from π^0 decays, the dominant source of background is expected to be pairs of such photons. The expected number of background pairs can be estimated by selecting all π^0 candidates based on their diphoton mass, and forming pairs of photons from among the π^0 daughters. Photons from less abundant η decays must be included as well. Photons from final-state radiation can be effectively rejected with a minimal energy requirement. In addition, the detailed $m_{\gamma\gamma}$ distribution for photon pairs arising from π^0 and η decays can be studied in samples of these mesons selected in charm meson decays, particularly $D \rightarrow K\pi^0$ and $D \rightarrow K\eta$.

IV. RESULTS AND DISCUSSION

In this section, we estimate the sensitivity of Belle II for detecting the processes $B \rightarrow Ka(3\pi)$ and $B \rightarrow Ka(\gamma\gamma)$ channels. We assume that 5×10^{10} pairs of $B\bar{B}$ are produced given the integrated luminosity of 50 ab^{-1} .

For the background-free $a \rightarrow 3\pi$ channel, we take the projected 95% confidence-level exclusion region in the plane of f_a vs m_a to be that for which the number of signal events satisfies $N_S \geq 3$. This region is shaded blue in Fig. 4.

For the $a \rightarrow \gamma\gamma$ final state, the projected 95% exclusion region is determined from $N_S/\sqrt{N_B}$, where N_B is the estimated number of background events given in section III B. Note that, since the sensitivity on f_a scales as $N_B^{1/4}$, the rough background estimation suffices for a relatively robust sensitivity estimate. The excluded region is shaded green in Fig. 4.

The projected sensitivities in Fig. 4 are shown for two different UV scales, $\Lambda_{\text{UV}} = 1$ TeV and $\Lambda_{\text{UV}} = 10$ TeV. The limits are tighter for higher choices of the UV scale because of large logarithmic corrections coming from the renormalization group evolution. We find that the dependence on the exact nature of the UV model, parametrized by the coefficients A and B in Ref. [42], is not important. The variation of A and B have sizeable effects only for $\Lambda_{\text{UV}} = 1$ TeV. Even in this case it is relevant only for the $m_a > 400$ MeV region for $a \rightarrow \gamma\gamma$ with at most $O(1)$ variation in f_a . To avoid clutter in Fig. 4, we choose optimistic values, $A = +3$ and $B = -3$.

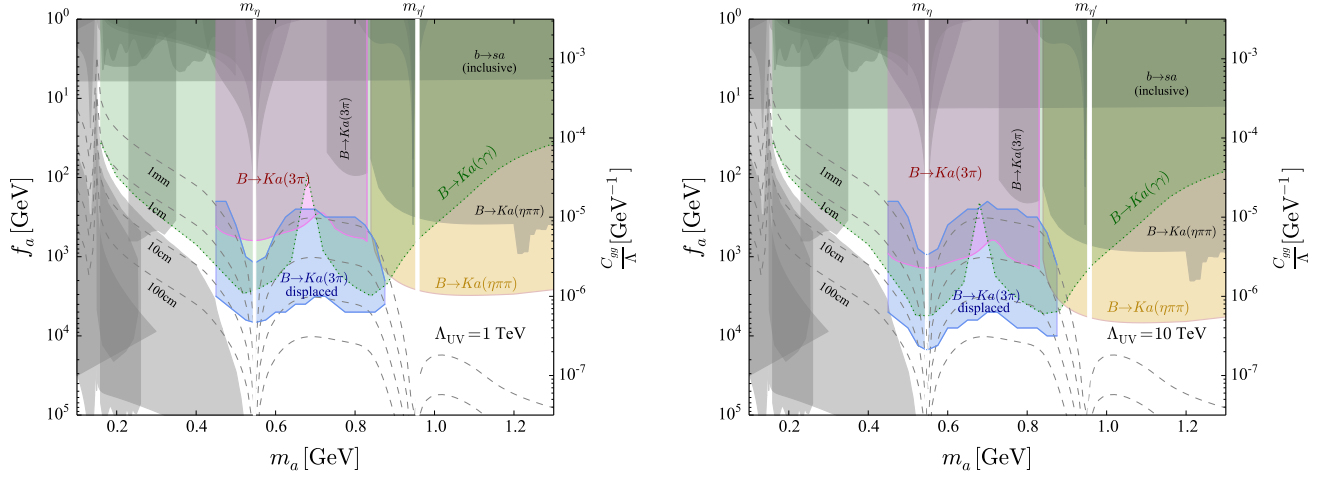


FIG. 4. In colors, we show the projected sensitivities for $\Lambda_{UV} = 1$ TeV (left figure) and 10 TeV (right figure) respectively, using prompt and displaced analysis. The projections developed in this paper are the $B \rightarrow Ka(3\pi)$ displaced analysis (blue region) and $B \rightarrow Ka(\gamma\gamma)$ prompt analysis (green region). The projections of $B \rightarrow Ka(3\pi)$ prompt analysis (magenta region) and $B \rightarrow Ka(3\pi)$ prompt analysis (yellow region) are from Ref. [42]. The grey regions refer to the present limits from B -decays, light meson decays and beam dump experiments. The dashed contours show the axion's $c\tau$ values.

To summarize, we find that for axion mass in the range $450 \lesssim m_a \lesssim 900$ MeV, the decay $a \rightarrow 3\pi$ with a displaced-vertex signature at Belle II is the best search channel, with sensitivities to the axion decay constant in the range $10^2 \lesssim f_a \lesssim 10^4$ GeV. Moreover, the $a \rightarrow \gamma\gamma$ channel can be used to probe the mass range $150 \lesssim m_a \lesssim 500$ MeV, covering the unconstrained range $10 \lesssim f_a \lesssim 10^3$ GeV of decay constant values.

ACKNOWLEDGMENTS

SC, VL, TO, and KT are supported by the US Department of Energy grant DE-SC0010102. TO and KT are also supported in part by JSPS KAKENHI 21H01086. EB and AS are supported by grants from the Israel Science Foundation, the US-Israel Binational Science Fund, the Israel Ministry of Science, and the Tel Aviv University Center for AI and Data Science.

-
- [1] S. Weinberg, “A New Light Boson?,” *Phys. Rev. Lett.* **40** (1978) 223–226.
 - [2] F. Wilczek, “Problem of Strong P and T Invariance in the Presence of Instantons,” *Phys. Rev. Lett.* **40** (1978) 279–282.
 - [3] R. Peccei and H. R. Quinn, “CP Conservation in the Presence of Instantons,” *Phys. Rev. Lett.* **38** (1977) 1440–1443.
 - [4] R. Peccei and H. R. Quinn, “Constraints Imposed by CP Conservation in the Presence of Instantons,” *Phys. Rev. D* **16** (1977) 1791–1797.
 - [5] G. ’t Hooft, “Symmetry Breaking Through Bell-Jackiw Anomalies,” *Phys. Rev. Lett.* **37** (1976) 8–11.
 - [6] P. Agrawal and K. Howe, “Factoring the Strong CP Problem,” *JHEP* **12** (2018) 029, [arXiv:1710.04213 \[hep-ph\]](#).
 - [7] M. Kamionkowski and J. March-Russell, “Planck scale physics and the Peccei-Quinn mechanism,” *Phys. Lett. B* **282** (1992) 137–141, [arXiv:hep-th/9202003](#).
 - [8] R. Holman, S. D. H. Hsu, T. W. Kephart, E. W. Kolb, R. Watkins, and L. M. Widrow, “Solutions to the strong CP problem in a world with gravity,” *Phys. Lett. B* **282** (1992) 132–136, [arXiv:hep-ph/9203206](#).
 - [9] S. M. Barr and D. Seckel, “Planck scale corrections to axion models,” *Phys. Rev. D* **46** (1992) 539–549.
 - [10] S. Ghigna, M. Lusignoli, and M. Roncadelli, “Instability of the invisible axion,” *Phys. Lett. B* **283** (1992) 278–281.
 - [11] J. Bjorken, S. Ecklund, W. Nelson, A. Abashian, C. Church, B. Lu, L. Mo, T. Nunamaker, and P. Rassmann, “Search for Neutral Metastable Penetrating Particles Produced in the SLAC Beam Dump,” *Phys. Rev. D* **38** (1988) 3375.
 - [12] J. Blumlein *et al.*, “Limits on neutral light scalar and pseudoscalar particles in a proton beam dump experiment,” *Z. Phys. C* **51** (1991) 341–350.
 - [13] **CHARM** Collaboration, F. Bergsma *et al.*, “Search for Axion Like Particle Production in 400-{GeV} Proton - Copper Interactions,” *Phys. Lett. B* **157** (1985) 458–462.
 - [14] **CAST** Collaboration, V. Anastassopoulos *et al.*, “New CAST Limit on the Axion-Photon Interaction,” *Nature Phys.* **13** (2017) 584–590, [arXiv:1705.02290 \[hep-ex\]](#).
 - [15] G. G. Raffelt, “Astrophysical axion bounds,” *Lect. Notes Phys.* **741** (2008) 51–71, [arXiv:hep-ph/0611350](#).

- [16] G. Raffelt, *Stars as laboratories for fundamental physics: The astrophysics of neutrinos, axions, and other weakly interacting particles*. 5, 1996.
- [17] A. Friedland, M. Giannotti, and M. Wise, “Constraining the Axion-Photon Coupling with Massive Stars,” *Phys. Rev. Lett.* **110** no. 6, (2013) 061101, [arXiv:1210.1271 \[hep-ph\]](#).
- [18] H. Fukuda, K. Harigaya, M. Ibe, and T. T. Yanagida, “Model of visible QCD axion,” *Phys. Rev. D* **92** no. 1, (2015) 015021, [arXiv:1504.06084 \[hep-ph\]](#).
- [19] P. Agrawal, G. Marques-Tavares, and W. Xue, “Opening up the QCD axion window,” *JHEP* **03** (2018) 049, [arXiv:1708.05008 \[hep-ph\]](#).
- [20] M. K. Gaillard, M. B. Gavela, R. Houtz, P. Quilez, and R. Del Rey, “Color unified dynamical axion,” *Eur. Phys. J. C* **78** no. 11, (2018) 972, [arXiv:1805.06465 \[hep-ph\]](#).
- [21] T. Gherghetta, V. V. Khoze, A. Pomarol, and Y. Shirman, “The Axion Mass from 5D Small Instantons,” *JHEP* **03** (2020) 063, [arXiv:2001.05610 \[hep-ph\]](#).
- [22] F. Takahashi and W. Yin, “Heavy QCD axion inflation,” [arXiv:2105.10493 \[hep-ph\]](#).
- [23] D. Aloni, Y. Soreq, and M. Williams, “Coupling QCD-Scale Axionlike Particles to Gluons,” *Phys. Rev. Lett.* **123** no. 3, (2019) 031803, [arXiv:1811.03474 \[hep-ph\]](#).
- [24] H. Georgi, D. B. Kaplan, and L. Randall, “Manifesting the Invisible Axion at Low-energies,” *Phys. Lett. B* **169** (1986) 73–78.
- [25] W. A. Bardeen, R. D. Peccei, and T. Yanagida, “CONSTRAINTS ON VARIANT AXION MODELS,” *Nucl. Phys. B* **279** (1987) 401–428.
- [26] D. S. M. Alves and N. Weiner, “A viable QCD axion in the MeV mass range,” *JHEP* **07** (2018) 092, [arXiv:1710.03764 \[hep-ph\]](#).
- [27] S. Gori, G. Perez, and K. Tobioka, “KOTO vs. NA62 Dark Scalar Searches,” *JHEP* **08** (2020) 110, [arXiv:2005.05170 \[hep-ph\]](#).
- [28] **E949** Collaboration, A. V. Artamonov *et al.*, “Search for the decay K^+ to π^+ gamma gamma in the π^+ momentum region $P > 213$ MeV/c,” *Phys. Lett. B* **623** (2005) 192–199, [arXiv:hep-ex/0505069](#).
- [29] **NA62** Collaboration, C. Lazzeroni *et al.*, “Study of the $K^\pm \rightarrow \pi^\pm \gamma \gamma$ decay by the NA62 experiment,” *Phys. Lett. B* **732** (2014) 65–74, [arXiv:1402.4334 \[hep-ex\]](#).
- [30] **KTeV** Collaboration, E. Abouzaid *et al.*, “Final Results from the KTeV Experiment on the Decay $K_L \rightarrow \pi^0 \gamma \gamma$,” *Phys. Rev. D* **77** (2008) 112004, [arXiv:0805.0031 \[hep-ex\]](#).
- [31] **KOTO** Collaboration, J. K. Ahn *et al.*, “Search for the $K_L \rightarrow \pi^0 \nu \bar{\nu}$ and $K_L \rightarrow \pi^0 X^0$ decays at the J-PARC KOTO experiment,” *Phys. Rev. Lett.* **122** no. 2, (2019) 021802, [arXiv:1810.09655 \[hep-ex\]](#).
- [32] M. Bauer, M. Neubert, S. Renner, M. Schnubel, and A. Thamm, “Consistent treatment of axions in the weak chiral Lagrangian,” [arXiv:2102.13112 \[hep-ph\]](#).
- [33] **PIENU** Collaboration, A. Aguilar-Arevalo *et al.*, “Search for heavy neutrinos in $\pi \rightarrow \mu \nu$ decay,” *Phys. Lett. B* **798** (2019) 134980, [arXiv:1904.03269 \[hep-ex\]](#).
- [34] D. Pocanic *et al.*, “Precise measurement of the $\pi^+ \rightarrow \pi^0 e^+ \nu$ branching ratio,” *Phys. Rev. Lett.* **93** (2004) 181803, [arXiv:hep-ex/0312030](#).
- [35] W. Altmannshofer, S. Gori, and D. J. Robinson, “Constraining axionlike particles from rare pion decays,” *Phys. Rev. D* **101** no. 7, (2020) 075002, [arXiv:1909.00005 \[hep-ph\]](#).
- [36] **GlueX** Collaboration, H. Al Gholi *et al.*, “Measurement of the beam asymmetry Σ for π^0 and η photoproduction on the proton at $E_\gamma = 9$ GeV,” *Phys. Rev. C* **95** no. 4, (2017) 042201, [arXiv:1701.08123 \[nucl-ex\]](#).
- [37] D. Aloni, C. Fanelli, Y. Soreq, and M. Williams, “Photoproduction of Axionlike Particles,” *Phys. Rev. Lett.* **123** no. 7, (2019) 071801, [arXiv:1903.03586 \[hep-ph\]](#).
- [38] **OPAL** Collaboration, G. Abbiendi *et al.*, “Multiphoton production in $e^+ e^-$ collisions at $s^{1/2} = 181$ -GeV to 209-GeV,” *Eur. Phys. J. C* **26** (2003) 331–344, [arXiv:hep-ex/0210016](#).
- [39] S. Knapen, T. Lin, H. K. Lou, and T. Melia, “Searching for Axionlike Particles with Ultraperipheral Heavy-Ion Collisions,” *Phys. Rev. Lett.* **118** no. 17, (2017) 171801, [arXiv:1607.06083 \[hep-ph\]](#).
- [40] **CMS** Collaboration, A. M. Sirunyan *et al.*, “Search for low mass vector resonances decaying into quark-antiquark pairs in proton-proton collisions at $\sqrt{s} = 13$ TeV,” *JHEP* **01** (2018) 097, [arXiv:1710.00159 \[hep-ex\]](#).
- [41] A. Mariotti, D. Redigolo, F. Sala, and K. Tobioka, “New LHC bound on low-mass diphoton resonances,” *Phys. Lett. B* **783** (2018) 13–18, [arXiv:1710.01743 \[hep-ph\]](#).
- [42] S. Chakraborty, M. Kraus, V. Loladze, T. Okui, and K. Tobioka, “Heavy QCD Axion in $b \rightarrow s$ transition: Enhanced Limits and Projections,” [arXiv:2102.04474 \[hep-ph\]](#).
- [43] **Particle Data Group** Collaboration, M. Tanabashi *et al.*, “Review of Particle Physics,” *Phys. Rev. D* **98** no. 3, (2018) 030001.
- [44] P. Ball and R. Zwicky, “ $B_{d,s} \rightarrow \rho, \omega, K^*, \phi$ decay form-factors from light-cone sum rules revisited,” *Phys. Rev. D* **71** (2005) 014029, [arXiv:hep-ph/0412079](#).
- [45] P. Ball and R. Zwicky, “New results on $B \rightarrow \pi, K, \eta$ decay formfactors from light-cone sum rules,” *Phys. Rev. D* **71** (2005) 014015, [arXiv:hep-ph/0406232](#).
- [46] E. Izaguirre, T. Lin, and B. Shuve, “Searching for Axionlike Particles in Flavor-Changing Neutral Current Processes,” *Phys. Rev. Lett.* **118** no. 11, (2017) 111802, [arXiv:1611.09355 \[hep-ph\]](#).
- [47] B. Batell, M. Pospelov, and A. Ritz, “Multi-lepton Signatures of a Hidden Sector in Rare B Decays,” *Phys. Rev. D* **83** (2011) 054005, [arXiv:0911.4938 \[hep-ph\]](#).
- [48] **BaBar** Collaboration, J. P. Lees *et al.*, “Search for $B \rightarrow K^{(*)} \nu \bar{\nu}$ and invisible quarkonium decays,” *Phys. Rev. D* **87** no. 11, (2013) 112005, [arXiv:1303.7465 \[hep-ex\]](#).
- [49] **BaBar** Collaboration, J. P. Lees *et al.*, “Search for Long-Lived Particles in $e^+ e^-$ Collisions,” *Phys. Rev. Lett.* **114** no. 17, (2015) 171801, [arXiv:1502.02580 \[hep-ex\]](#).
- [50] **Belle** Collaboration, D. Liventsev *et al.*, “Search for heavy neutrinos at Belle,” *Phys. Rev. D* **87** no. 7, (2013) 071102, [arXiv:1301.1105 \[hep-ex\]](#). [Erratum: *Phys.Rev.D* 95, 099903 (2017)].
- [51] L. Lee, C. Ohm, A. Soffer, and T.-T. Yu, “Collider Searches for Long-Lived Particles Beyond the Standard

- Model,” *Prog. Part. Nucl. Phys.* **106** (2019) 210–255, [arXiv:1810.12602 \[hep-ph\]](#).
- [52] J. Alimena *et al.*, “Searching for long-lived particles beyond the Standard Model at the Large Hadron Collider,” *J. Phys. G* **47** no. 9, (2020) 090501, [arXiv:1903.04497 \[hep-ex\]](#).
- [53] **Belle** Collaboration, V. Chobanova *et al.*, “Measurement of branching fractions and CP violation parameters in $B \rightarrow \omega K$ decays with first evidence of CP violation in $B^0 \rightarrow \omega K_S^0$,” *Phys. Rev. D* **90** no. 1, (2014) 012002, [arXiv:1311.6666 \[hep-ex\]](#).
- [54] D. J. Lange, “The EvtGen particle decay simulation package,” *Nucl. Instrum. Meth. A* **462** (2001) 152–155.
- [55] C. O. Dib, J. C. Helo, M. Nayak, N. A. Neill, A. Soffer, and J. Zamora-Saa, “Searching for a sterile neutrino that mixes predominantly with ν_τ at B factories,” *Phys. Rev. D* **101** no. 9, (2020) 093003, [arXiv:1908.09719 \[hep-ph\]](#).
- [56] S. Dey, C. O. Dib, J. Carlos Helo, M. Nayak, N. A. Neill, A. Soffer, and Z. S. Wang, “Long-lived light neutralinos at Belle II,” *JHEP* **02** (2021) 211, [arXiv:2012.00438 \[hep-ph\]](#).
- [57] **Belle** Collaboration, Y. T. Duh *et al.*, “Measurements of branching fractions and direct CP asymmetries for $B \rightarrow K\pi$, $B \rightarrow \pi\pi$ and $B \rightarrow KK$ decays,” *Phys. Rev. D* **87** no. 3, (2013) 031103, [arXiv:1210.1348 \[hep-ex\]](#).
- [58] **BaBar** Collaboration, B. Aubert *et al.*, “B meson decays to charmless meson pairs containing eta or eta’ mesons,” *Phys. Rev. D* **80** (2009) 112002, [arXiv:0907.1743 \[hep-ex\]](#).
- [59] **Belle** Collaboration, C. T. Hoi *et al.*, “Evidence for Direct CP Violation in $B^\pm \rightarrow \eta h^\pm$ and Observation of $B^0 \rightarrow \eta K^0$,” *Phys. Rev. Lett.* **108** (2012) 031801, [arXiv:1110.2000 \[hep-ex\]](#).
- [60] **Belle** Collaboration, Y. T. Duh *et al.*, “Measurements of branching fractions and direct CP asymmetries for $B \rightarrow K\pi$, $B \rightarrow \pi\pi$ and $B \rightarrow KK$ decays,” *Phys. Rev. D* **87** no. 3, (2013) 031103, [arXiv:1210.1348 \[hep-ex\]](#).
- [61] **BaBar** Collaboration, “Belle ii $m_{\gamma\gamma}$ plots,” <https://docs.belle2.org/record/1589/files/BELLE2-NOTE-PL-2019-019.pdf>.
- [62] **BaBar** Collaboration, J. P. Lees *et al.*, “Search for the Decay $D^0 \rightarrow \gamma\gamma$ and Measurement of the Branching Fraction for $D^0 \rightarrow \pi^0\pi^0$,” *Phys. Rev. D* **85** (2012) 091107, [arXiv:1110.6480 \[hep-ex\]](#).